PAPER

Cytotoxic and antimicrobial indole alkaloids from an endophytic fungus *Chaetomium* sp. SYP-F7950 of *Panax notoginseng*†

Fei Peng,[ab] Shao-Yang Hou,[a] Tian-Yuan Zhang,[a] Ying-Ying Wu,[a] Meng-Yue Zhang,[a] Xi-Meng Yan,[a] Ming-Yu Xia[a] and Yi-Xuan Zhang [ID] *[a]

Two new compounds chetoseminudin F (**1**) and G (**2**) together with eleven known compounds were isolated from the solid fermentation products of the endophytic fungus *Chaetomium* sp. SYP-F7950. The structures of the isolated compounds were elucidated by extensive spectroscopic analyses, including 1D and 2D NMR, and HRFABMS experiments. The absolute configurations of chetoseminudin F (**1**) and G (**2**) were determined by comparing the electronic circular dichroism (ECD) spectrum with those of the reported references. A plausible biogenetic pathway for compounds **1–6** and **9–13** was proposed. These isolates were also evaluated for their antimicrobial and antitumor activity, revealing that chetoseminudin F (**1**) displayed more potent cytotoxicity against MDA-MB-231 cells with an IC_{50} value of 26.49 μmol L^{-1} more than the common chemotherapeutic agent (paclitaxel). In antimicrobial assay, compounds **6**, **9**, **11** and **12** had strong antibacterial activity against *Staphylococcus aureus*, *Bacillus subtilis*, *Enterococcus faecium* and antifungal activity against *Candida albicans* with minimum inhibitory concentration (MIC) values ranging from 0.12 to 9.6 μg mL^{-1}; meanwhile compounds **6**, **8**, **9** and **12** exhibited strong cytotoxicity with IC_{50} values of 2.75–8.68 μmol L^{-1} against tumor cell lines A549 and MDA-MB-231. In addition, morphological observation showed that treatment with compounds **6**, **9** and **12** increased the mean length of *B. subtilis* by 1.6 to 1.8-fold. *In silico* molecular docking was applied to study the binding interactions between the compounds and the active sites of filamentous temperature-sensitive protein Z (FtsZ) from *B. subtilis*. Compounds **6**, **9** and **12** displayed the low binding energies, strong H-bond interactions with FtsZ. On the basis of the antimicrobial activities, cellular phenotype observation and docking studies, compounds **6**, **9** and **12** are considered to be a promising antimicrobial inhibitor of FtsZ.

Introduction

Chaetomium, which includes about 400 species in the Index Fungorum (http://www.indexfungorum.org/Names/Names.asp) since Kunze first established this genus in 1817,[1] is one of the largest genera in Chaetomiaceae family.[1] It is widely distributed in different biotopes, such as soil, marine, animal dung, hair, textile, plant seeds and some other substrates being rich in cellulose. Thus, *Chaetomium* spp. are often used to produce cellulose in industry, and are also used as biocontrol agents in agriculture. Since chaetomin was firstly reported from *Chaetomium* sp. in 1944,[2] a wide variety of compounds have been reported in this genus such as armochaetoglobins A–J,[3] xanthenone,[4] chaetoglobins,[5] and

orsellides,[6] some of which showed interesting biological activities including cytotoxic, antibacterial, antifungal and anti-inflammatory activities.[7–9]

Panax notoginseng F. H. Chen (Araliaceae) is a valued traditional Chinese medicinal herb,[10] which as a perennial plant should be grown in the field for at least three years to obtain high-quality raw roots.[11] *P. notoginseng* is vulnerable to be attacked by soil-borne pathogens including fungi, bacteria, and nematodes due to the required long-term continuous cultivation.[12,13] Endophytic fungi play a key role in plant defense and could be used as a promising source for biocontrol agents.[14] There is little doubt that secondary metabolites of endophytic fungi play important roles in the antagonism against many pathogens.[15,16] As part of our ongoing researches to discovery for new bioactive metabolites from endophytic fungi from *P. notoginseng*,[17–19] a fungus, *Chaetomium* sp. SYP-F7950, was isolated from the stem of *Panax notoginseng* collected in Wenshan district of Yunnan province of China. The large-scale fermentation followed by combinatorial chromatography led to isolation of two new compounds, chetoseminudin F (**1**) and

[a]School of Life Science and Biopharmaceutics, Shenyang Pharmaceutical University, Shenyang 110016, PR China. E-mail: zhangyxzsh@163.com

[b]Quanzhou Medical College, Quanzhou, PR China

1. $R_1=OCH_3$ $R_2=CH_3$
2. $R_1=OCH_3$ $R_2=H$
3. $R_1=SCH_3$ $R_2=CH_3$
4. $R_1=SCH_3$ $R_2=H$
5. $R_1=OH$ $R_2=CH_3$
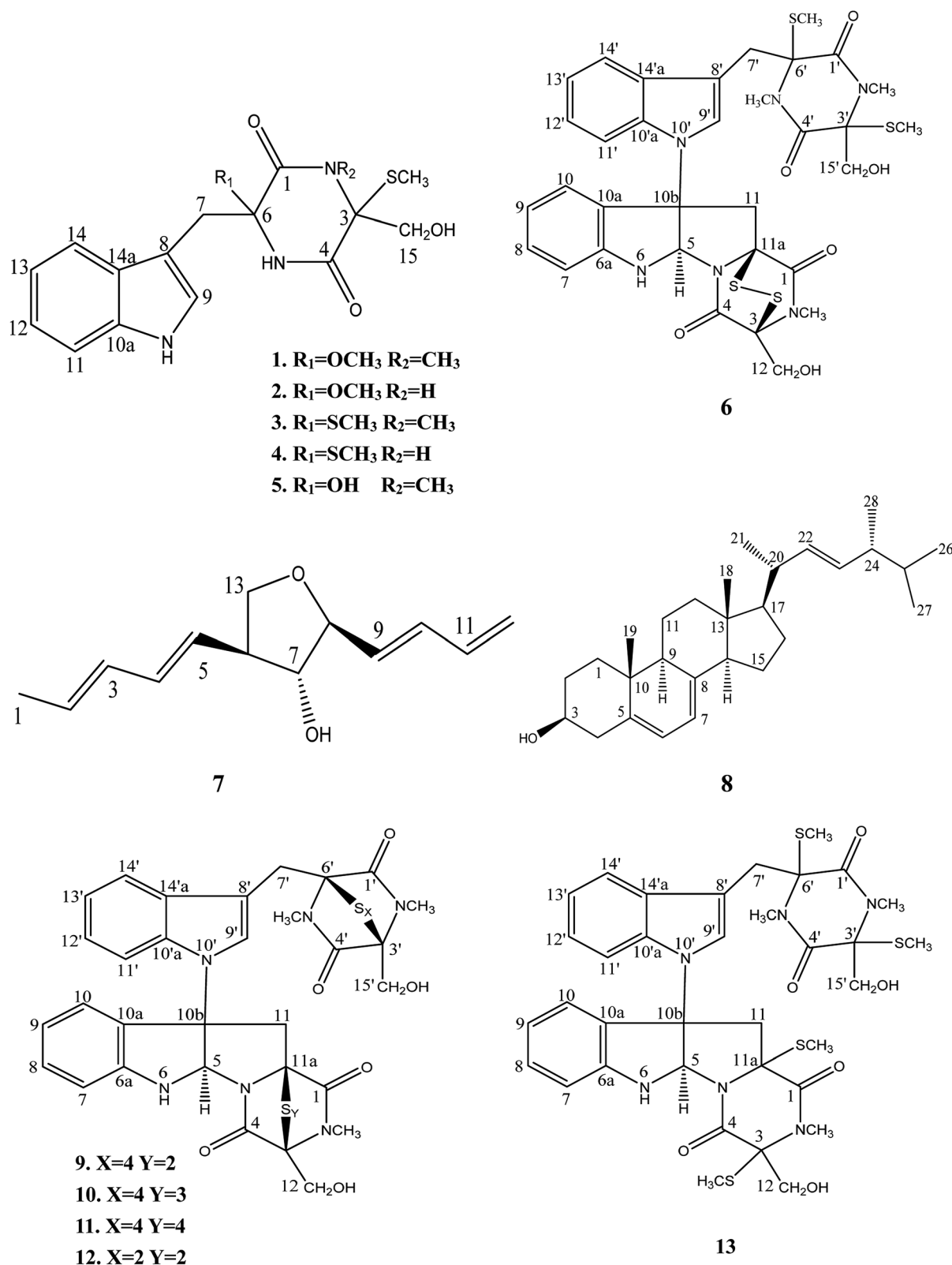
9. X=4 Y=2
10. X=4 Y=3
11. X=4 Y=4
12. X=2 Y=2

Fig. 1 Chemical structure of compounds **1–13** isolated from *Chaetomium* sp. SYP-F7950.

chetoseminudin G (**2**), together with eleven known compounds (**3–13**) (Fig. 1). Meanwhile, a plausible biogenetic pathway for compounds **1–6** and **9–13** was proposed. Therefore, the aims of this study are to discover the diversity of endophytic fungi of *P. notoginseng* and to obtain antimicrobial secondary metabolites from this strain.
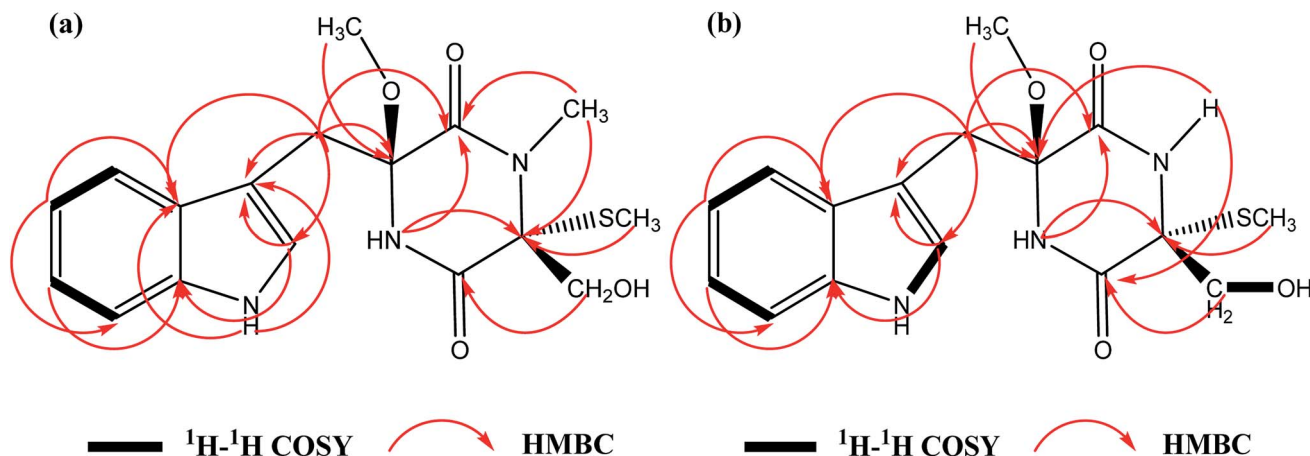
Fig. 2 Key 2D correlations of chetoseminudin F (**1**, a) and G (**2**, b).

The rise and rapid spread of antibiotic resistance renders it necessary to discovery novel targets and new drug classes. In recent years, bacterial cell division has attracted considerable attention as a potential target pathway for antibiotic treatment. FtsZ is considered to be the major protein of the bacterial cell division machinery (divisome).[20,21] FtsZ is an appealing target for new antibacterial drug discovery due to several key reasons. First, it is an essential protein for bacterial viability.[22] Second, FtsZ protein is a potentially broad-spectrum antibacterial target because it is highly conserved and has been identified in most bacteria. Third, FtsZ is not present in higher eukaryotes,[23] which suggests that FtsZ inhibitors should not be toxic to human cells. All of these suggests that FtsZ may be amenable to inhibitor development. In our study, three indole alkaloids were identified as potential inhibitors of FtsZ by morphological observation and molecular docking, which explore the possible binding mechanism between the lead compounds and FtsZ.

Results and discussion

Compound **1** was obtained as a yellow powder. The UV spectrum of compound **1** gave the absorption of an indole system (274, 281, and 290 nm) (Fig. S10†), and the IR spectrum showed the absorption of OH and NH (3380 and 3225 cm^{-1}), CH$_3$ (2923 cm^{-1}) and amide $>$C$=$O groups (1641 cm^{-1}) (Fig. S12†). The molecular formula of **1** was calculated to be C$_{17}$H$_{21}$N$_3$O$_4$S with the molecular weight of m/z 386.1148 [M + Na]$^+$ (calcd for 386.1145) by HRFABMS with 8 degrees of unsaturation. The ^{1}H

Table 1 ^{1}H (600 MHz) and ^{13}C NMR (150 MHz) spectral data of **1** and **2** in DMSO-d_6

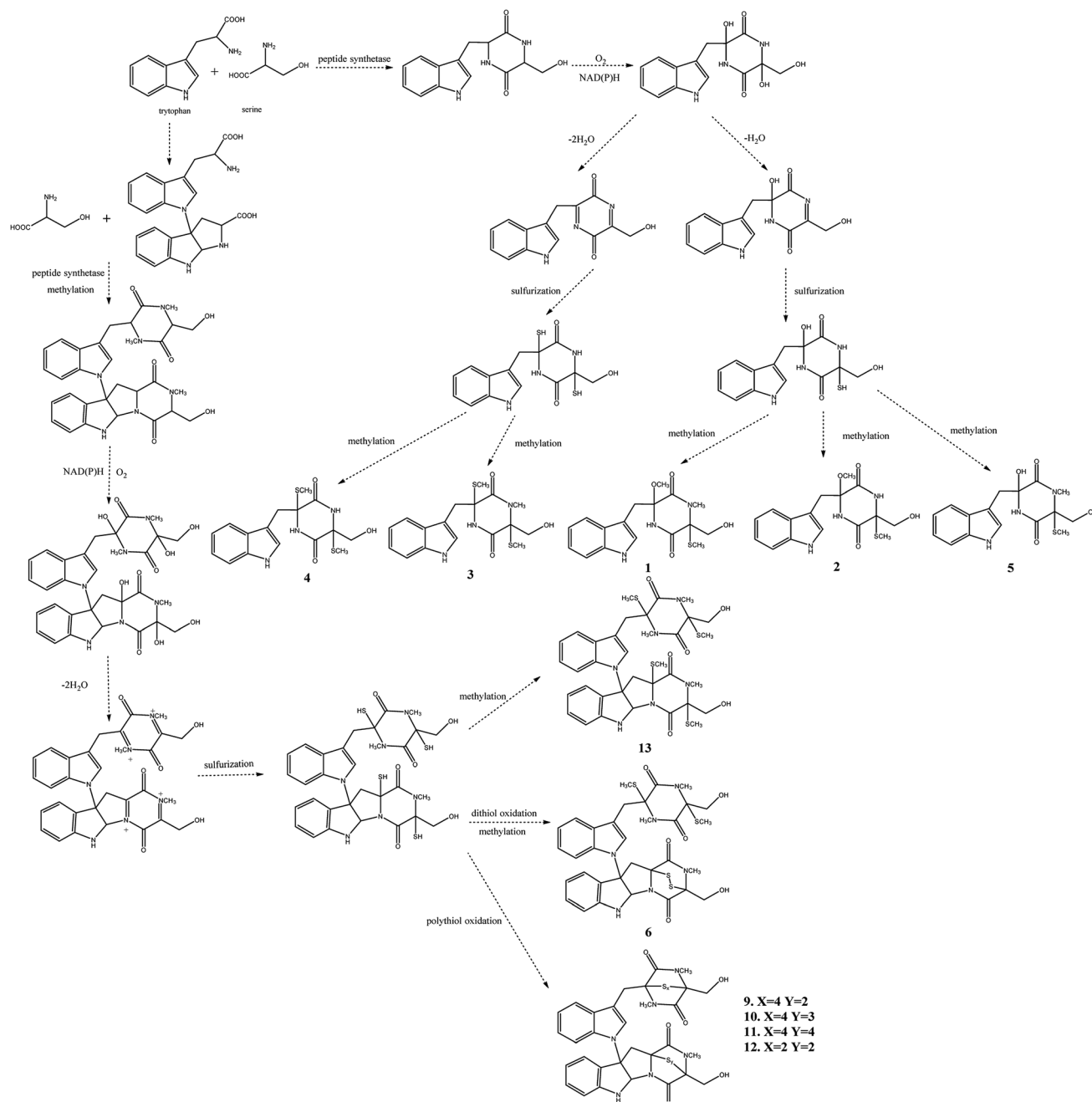|	Compound **1**			Compound **2**	
Position	δ_C, type	δ_H (J in Hz)	Position	δ_C, type	δ_H (J in Hz)
1	165.0 C	—	1	165.3 C	—
2 NCH$_3$	28.3 CH$_3$	2.80, s, 3H	2 NH	—	8.68, s, 1H
3	75.2 C	—	3	67.8 C	—
3 SCH$_3$	8.3 CH$_3$	0.43, s, 3H	3 SCH$_3$	9.7 CH$_3$	0.87, s, 3H
4	165.5 C	—	4	165.9 C	—
5 NH	—	9.00, s, 1H	5 NH	—	8.72, s, 1H
6	87.6 C	—	6	87.7 C	—
6 OCH$_3$	50.9 CH$_3$	3.17, s, 3H	6 OCH$_3$	50.8 CH$_3$	3.18, s, 3H
7	35.2 CH$_2$	3.02, d, 1H, 12 3.49, d, 1H, 12	7	34.6 CH$_2$	2.99, d, 1H, 12 3.43, d, 1H, 12
8	107.3 C	—	8	107.0 C	—
9	125.4 CH	7.04, d, 1H, 6	9	125.6 CH	7.06, d, 1H, 6
10 NH	—	10.92, s, 1H	10 NH	—	10.91, s, 1H
10a	135.9 C	—	10a	135.9 C	—
11	111.1 CH	7.26, d, 1H, 6	11	111.1 CH	7.26, d, 1H, 6
12	120.8 CH	7.01, t, 1H, 6	12	120.8 CH	7.00, t, 1H, 6
13	118.4 CH	6.94, t, 1H, 6	13	118.8 CH	6.94, t, 1H, 6
14	118.9 CH	7.67, d, 1H, 6	14	119.0 CH	7.67, d, 1H, 6
14a	128.2 C	—	14a	128.2 C	—
15	62.8 CH$_2$	3.42, d, 1H, 12 3.73, d, 1H, 12	15	65.3 CH$_2$	3 28, d, 1H, 12 3.69, d, 1H, 12

Fig. 3 Proposed biosynthetic pathway for compounds **1–6** and **9–13**.

NMR and ^{13}C NMR spectral data of **1** (Table 1) revealed 17 carbons, including 3 methyl groups, 2 methylenes, 5 methines and 7 quaternary carbons. A comparison of the spectroscopic data between **1** and chetoseminudin E[24] indicated their similarities except that compound **1** possessed a CH_3–O group (δ_H 3.17; δ_C 50.9) at 6 position instead of –OH group in chetoseminudin E, which was further confirmed by the long-range HMBC correlations from CH_3–O (δ_H 3.17) to C6 (δ_C 87.6). In the NMR spectra of **1**, three CH_3 signals at δ_H/δ_C 2.80/28.3, 0.43/8.3 and 3.17/50.9 were assigned to CH_3–N, CH_3–S and CH_3–O, respectively, and the two CH_2 signals at δ_H/δ_C 3.02, 3.49/35.2

and 3.42, 3.73/62.8 were assigned to CH_2-7 and CH_2-15, respectively, by HMBC correlations (Fig. 2a) Examination of the ^{1}H and ^{13}C NMR spectra of **1** showed the presence of a 3-substituted indolyl group [δ_H 7.04 (1H, d, J = 6 Hz, H-9), 7.26 (1H, d, J = 6 Hz, H-11), 7.01 (1H, t, J = 6 Hz, H-12), 6.94 (1H, t, J = 6 Hz, H-13) and 7.67 (1H, d, J = 6 Hz, H-14); δ_C 107.3 (C, C-8), 125.4 (CH, C-9), 135.9 (C, C-10a), 111.1 (CH, C-11), 120.8 (CH, C-12), 118.4 (CH, C-13), 118.9 (CH, C-14) and 128.2 (C, C-14a)]. The long-range HMBC correlations from H-2 (NCH$_3$) to C-1 and C-3, H-3 (SCH$_3$) to C-3, H-15 to C-4, H-5 to C-1 and C-3, H-6 (OCH$_3$) to C6 revealed the presence of

Table 2 Inhibition effects of fungal metabolites on the growth of tumor cells *in vitro*[a]

	IC$_{50}$ (μmol L^{-1})	
	Cell line	
Substance no.	A549	MDA-MB-231
1	>30	26.49
2	>30	>30
3	>30	>30
4	>30	>30
5	20.81	>30
6	4.58	7.20
7	>30	>30
8	4.84	>30
9	8.68	>30
10	>30	>30
11	>30	>30
12	>30	2.75
13	15.66	22.30
Paclitaxel	<0.3	30.00

[a] The cells were cultured with various concentrations of different samples for 48 h.

a monothiodimethyldioxopiperazine moiety, as shown in Fig. 1. No NOESY correlations were observed to determine the relative configuration of 1. As shown in Fig. S11,† the absolute configuration of 1 was determined by comparing ECD spectrum with those of the reported references, revealing that the cotton effects in the experimental ECD spectrum of 1 were consistent with chetoseminudin E.[24] Thus, its absolute configuration was determined as 3R,6S. These data confirmed the chemical structure of compound 1, named as chetoseminudin F, as a new chetoseminudin alkaloid characterized by a 3-substituted indolone integrated with a monothiodimethyldioxopiperazine ring with methoxy-substituted at 6 position.

Compound 2 was obtained as a yellow powder. The molecular formula of compound 2 was determined to be C$_{16}$H$_{19}$N$_3$O$_4$S with the molecular weight of *m/z* 372.0982 [M + Na]$^+$ (calcd for 372.1096) by HRFABMS, indicating 8 degrees of unsaturation. The UV spectrum of 2 gave the absorption of an indole system (274, 281, and 290 nm) (Fig. S22†), and the IR spectrum of 2 showed the absorption of OH and NH (3419 cm^{-1}), CH$_3$ (2921 cm^{-1}) and amide $\rangle$C=O groups (1677 cm^{-1}) (Fig. S24†). The ^{1}H NMR and ^{13}C NMR spectral data of 2 (Table 1) showed that 2 was built up by a combination of a 3-methylindole and monothiodioxopiperazine moieties, and revealed 16 carbons, including 2 methyl groups, 2 methylenes, 5 methines and 7 quaternary carbons. Comparison of NMR spectra of 2 (Table 1) with those of 1 suggested that the CH$_3$–N group at position 2 (δ_H/δ_C 2.80/28.3) in 1 was replaced with an H–N group (δ_H 8.68) in 2, which was confirmed by the long-range HMBC correlations from H–N (δ_H 8.68) to C4 (δ_C 165.9) and C6 (δ_C 87.7). In the NMR spectra of 2, two CH$_3$ signals at δ_H/δ_C 0.87/9.7 and 3.18/50.8 were assigned to CH$_3$–S and CH$_3$–O, respectively, and the two CH$_2$ signals at δ_H/δ_C 2.99, 3.43/34.6 and 3.28, 3.69/65.3 were assigned to CH$_2$-7 and CH$_2$-15, respectively, by HMBC correlations (Fig. 2b). No NOESY correlations were observed to determine the relative configuration of 2. As shown in Fig. S20,† the absolute configuration of 2 was determined by comparing the electronic circular dichroism (ECD) spectrum with 1, revealing that the cotton effects in the experimental ECD spectrum of 2 were consistent with 1. Thus, its absolute configuration was determined as 3R,6S. All above data confirmed the chemical structure of compound 2 belonging to a new indole alkaloid, named as chetoseminudin G.

Eleven known compounds were identified to be chetoseminudin B (3)[25] (Table S1 and Fig. S25–S27†), chetoseminudin C (4)[26] (Table S5 and Fig. S28–S30†), chetoseminudin E (5)[24] (Table S1 and Fig. S31–S33†), chaetocochin C (6)[27] (Table S2 and Fig. S34–S36†), 3-*epi*-aureonitol (7)[28] (Table S3 and Fig. S37–S39†), ergosterol (8)[29] (Table S4 and Fig. S40–S42†), chetomin A

Table 3 MICs of fungal metabolites against bacteria and fungi

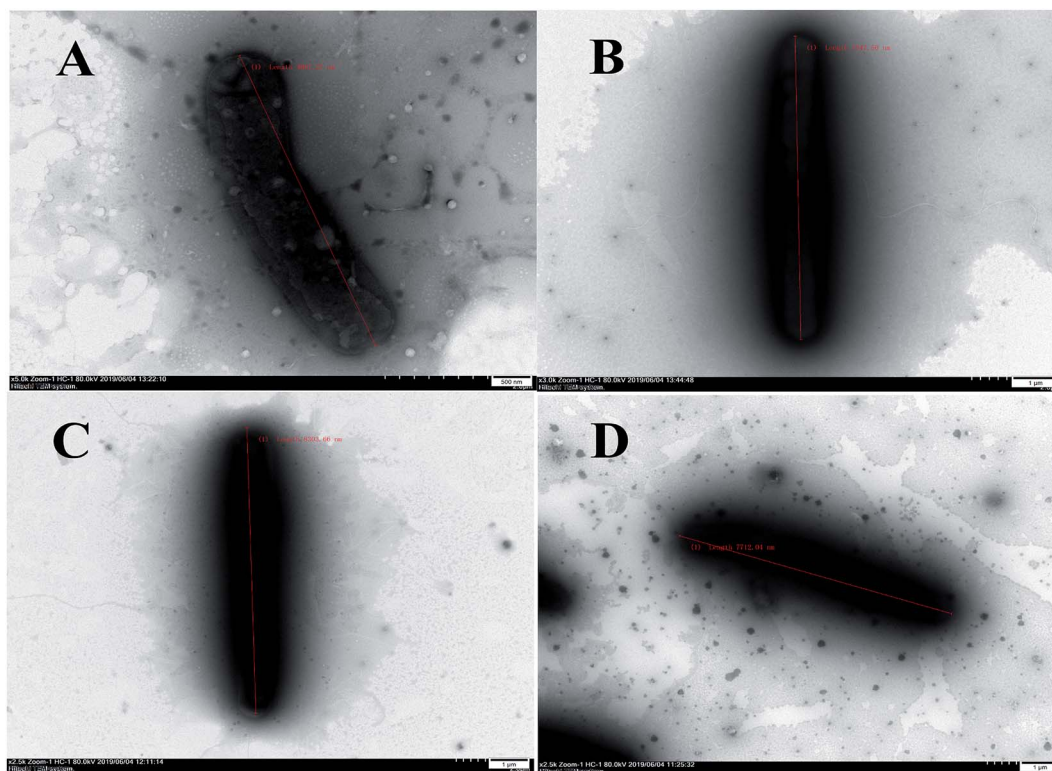| Compound (μg mL^{-1})	MICs (μg mL^{-1})							
	Staphylococcus aureus	*Bacillus subtilis*	*E. coli*	*Enterococcus faecium*	*Proteus mirabilis*	*Acinetobacter baumannii*	*Achromobacter marplatensis*	*Candida albicans*
1	>200	>200	>200	>200	>200	>200	76.7	124.1
2	>200	>200	>200	>200	>200	>200	117.7	103.3
3	>200	>200	>200	>200	>200	>200	>200	>200
4	>200	>200	>200	>200	>200	>200	>200	>200
5	>200	>200	>200	>200	>200	>200	>200	>200
6	0.5	0.25	>200	19.3	>200	>200	29.0	12.4
7	>200	>200	>200	>200	>200	>200	>200	>200
8	>200	>200	>200	>200	>200	>200	>200	>200
9	0.12	0.2	>200	3.6	>200	>200	165.8	20.4
10	65.2	30.5	>200	12.4	>200	>200	69.1	18.8
11	44.3	50.0	>200	4.1	>200	>200	41.8	8.3
12	4.3	2.4	>200	3.3	>200	>200	42.6	9.6
13	23.4	15.0	>200	37.3	>200	>200	43.3	12.6
Vancomycin	2.5	1.5	50.0	10.0	50.0	30.0	50.0	—
Geneticin	—	—	—	—	—	—	—	6.0

Fig. 4 Electron micrographs of *B. subtilis* in the absence or presence of compounds **6**, **9** and **12**. (A) Untreated control cells of *B. subtilis* with average length of 4.60 μm. (B–D) Filamentous cells of *B. subtilis* treated with compounds **6** (B), **9** (C) and **12** (D) showed average length of 7.35, 8.30 and 7.72 μm, respectively.

Table 4 Binding residues involved in the formation of hydrogen bonds with compounds **6**, **9** and **12** and ligands

| | | | Residues | |
| | | | | |
Compound	PDB (ID)	Docking score (kcal mol^{-1})	Conventional hydrogen bond	Carbon hydrogen bond
6	2VXY	−158	ARG143, GLY108, GLY110, THR109	GLY107
9	2VXY	−156	ALA71, ALA73, ASN44, THR109	ASP46
12	2VXY	−154	ALA71, ALA73, ASN25, GLY72	
Ligand	2VXY	−83	ALA71, ALA73, GLY21, GLY108, GLY110, THR109	GLY107

(**9**)[30] (Table S6 and Fig. S43–S45†), chetomin B[30] (**10**) (Table S6 and Fig. S46–S48†), chetomin C[30] (**11**) (Table S6 and Fig. S49–S51†), chetomin (**12**)[25] (Table S6 and Fig. S52–S54†) and dethiotetra-(methylthio)-chetomin (**13**)[27] (Table S6 and Fig. S55–S57†) by comparing their NMR data and ESI-MS with those reported (see in the ESI†).

The postulated biosynthetic pathway for compounds **1–6** and **9–13** is demonstrated in Fig. 3. For compounds **1–5**, all of them began with the condensation of serine and tryptophan by a nonribosomal peptide synthetase,[31] followed by C-hydroxyl-ation,[32] water elimination,[33] sulfurization[33] and O- or S-methyl-ation[34] to afford compounds **1–5**. For compounds **6** and **9–13**, they were derived from tryptophan-derived heterodimer *via* a radical dimerization,[35] followed by the peptide coupling reactions with serine and subsequent dioxopiperazine

cyclization by a nonribosomal peptide synthetase, N-methylation, water elimination, sulfurization, S-methylation and di or polythiol-oxidation to afford compounds **6** and **9–13** which has been reported previously.[31]

Seven test bacteria (*Staphylococcus aureus*, *Bacillus subtilis*, *Escherichia coli*, *Enterococcus faecium*, *Proteus mirabilis*, *Acinetobacter baumannii* and *Achromobacter marplatensis*) and one fungus (*Candida albicans*) were selected for antibacterial and antifungal assays (Table 3). In antimicrobial assay, compounds **1** and **2** showed weak inhibitory activity against *A. marplatensis* and *C. albicans* with MICs values of 117.7, 76.7, 103.3 and 124.1 μg mL^{-1} (vancomycin, MIC = 50 μg mL^{-1} and geneticin, MIC = 6.0 μg mL^{-1}), respectively. However, the above compounds were inactive against another six test microorganisms. At the same time, compounds **6**, **9** and **12**
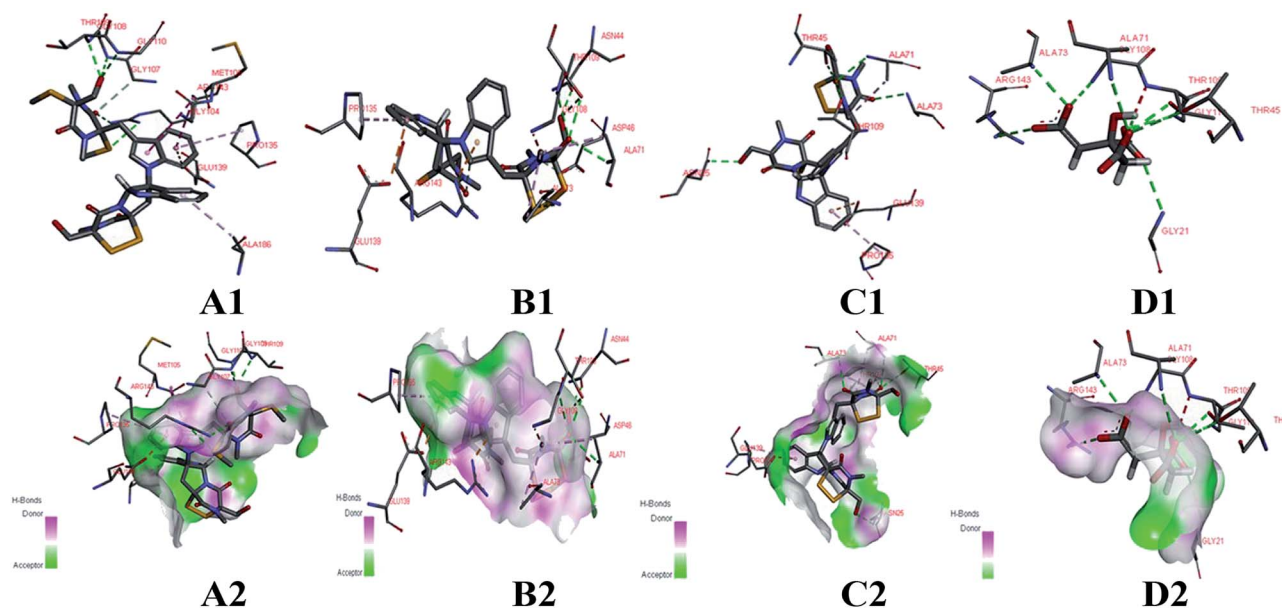
Fig. 5 Docking models of compounds **6**, **9**, **12** and ligand with FtsZ of *B. subtilis* (PDB ID: 2VXY). (A1, B1, C1 and D1) The binding sites of H-bond or hydrophobic between **6**, **9**, **12**, ligand and FtsZ. (A2, B2, C2 and D2) The 3D docking model with H-bond pocket between **6**, **9**, **12**, ligand and FtsZ.

exhibited strong inhibitor activities against *S. aureus* with MIC values of 0.5, 0.12, and 4.3 µg mL^{-1}, respectively. The above compounds also exhibited strong inhibitor activities against *B. subtilis* with MIC values of 0.25, 0.2 and 2.4 µg mL^{-1}, respectively. Compounds **9**, **11** and **12** also displayed strong antagonistic activities against *E. faecium* with MIC values of 3.6, 4.1 and 3.3 µg mL^{-1} respectively. In antifungal assay, compounds **11** and **12** significantly inhibited the growth of *C. albicans* with MIC values of 8.3 and 9.6 µg mL^{-1} respectively. In anticancer assay, compound **2** exhibited more potent cytotoxic effect against MDA-MB-231 cell with IC$_{50}$ value of 26.49 µmol L^{-1} than paclitaxel (Table 2). Meanwhile, compounds **6** and **12** showed obvious cytotoxic activity against MDA-MB-231 with IC$_{50}$ values of 7.20 and 2.75 µmol L^{-1}. Compounds **6**, **8** and **9** displayed obvious cytotoxic activity against A549 with IC$_{50}$ values of 4.58, 4.84 and 8.68 µmol L^{-1}.

The cells of *B. subtilis* treated with the compounds **6**, **9** and **12** were observed to study the possible antibacterial mechanism in more detail. Interestingly, as shown in Fig. 4, the rod-shaped cells of *B. subtilis* grew into longer filaments under the treatment of compounds **6**, **9** and **12**, which reached 1.6, 1.8 and 1.7-fold length of the untreated cells, respectively. To explain this interesting result, the filamentous temperature-sensitive protein Z (FtsZ), the key protein of cell division,[36] was applied to illustrate the mechanism of cells that became filamentous. Thus, a molecular docking study was conducted to validate the deduction. The docking results are shown in Table 4 and Fig. 5. The FtsZ from *B. subtilis* (PDB: ID 2VXY) displayed the docking score (Table 4) of **6**, **9** and **12** that were all lower than its ligand, thus indicating better binding abilities. Compound **6** displayed four conventional hydrogen bonds and one carbon hydrogen bonds with neighbouring amino acid residues. Compound **9** also displayed four

conventional hydrogen bonds and one carbon hydrogen bonds with neighbouring amino acid residues. The docking scores −158 kcal mol^{-1} (**6**) and −156 kcal mol^{-1} (**9**), indicate that two compounds may both form lower binding energy and stable binding sites with the target protein. Compound **12** formed four conventional hydrogen bonds with the ALA 71, ALA 73, ASN 25 and GLY 72 residues as listed in Table 4 and Fig. 5. In total, the docking results revealed that compounds **6**, **9** and **12** exhibited low binding energies, strong H-bond interactions with the FtsZ from *B. subtilis* to validate the phenotypic consequence and antimicrobial activity. Therefore, the morphological changes and *in silico* docking simulations provided strong proof that compounds **6**, **9** and **12** are potential inhibitors of FtsZ from *B. subtilis*.

Conclusion

This study resulted in isolation and identification of two new indole alkaloids, chetoseminudin F (**1**) and G (**2**), and eleven known compounds from *Chaetomium globosum* on the basis of 1D, 2D NMR, HRESIMS. The absolute configuration of chetoseminudin F (**1**) and G (**2**) were determined as 3*R*,6*S* by comparing the electronic circular dichroism (ECD) spectrum with chetoseminudin E.[24] In antimicrobial assays, compounds **6**, **9**, **11** and **12** had strong antibacterial activity against *Staphylococcus aureus*, *B. subtilis*, *Enterococcus faecium* and antifungal activity against *Candida albicans* with minimum inhibitory concentration (MIC) values ranging from 0.12 to 9.6 µg mL^{-1}. In antitumor assays, chetoseminudin G (**2**) displayed more potent cytotoxicity in MDA-MB-231 cells with IC$_{50}$ value of 26.49 µmol L^{-1} than the common chemotherapeutic agent (paclitaxel). Meanwhile, compounds **6**, **8**, **9** and **12** also exhibited strong cytotoxicity with IC$_{50}$ values of 2.75–8.68 µmol L^{-1} against cell

lines A549 and MDA-MB-231. TEM images indicated the mean length of *B. subtilis* increased under treatment with compounds **6**, **9** and **12**. In addition, these compounds showed low binding energies and strong H-bond interactions with the FtsZ from *B. subtilis*. These results revealed that the antimicrobial mechanism of these compounds against *B. subtilis* could be achieved by combination with FtsZ, resulting in the inhibition of cell division. On the basis of the antimicrobial activities, phenotypic consequences and docking studies, these indole alkaloids were identified to be a promising antimicrobial lead molecule. Our current findings would greatly expand the chemical and pharmacological diversities of the metabolites of *Chaetomium* species.

Experimental method

General experimental procedures

UV spectra were recorded on a Shimadzu UV 2201 spectrophotometer. ECD spectra were recorded on a Bio-Logic Science MOS-450 spectrometer. Bruker AV-600 spectrometer was used in the NMR experiments. Optical rotations were obtained on PerkinElmer 241. HRESIMS data were acquired on a Bruke TOF mass spectrometer. Preparative HPLC was performed on SHIMADZU 20A-DAD HPLC using Welch Materials Ultimate XB-C18 (5 μm) 10 × 250 mm column. Silica gel (200–300 mesh) was purchased from Qingdao Marine Chemical Factory (Qingdao, China). Size exclusion chromatography was done on Sephadex LH-20 (Amersham, GE in USA).

Fungal material

The fungal strain in this research was isolated from the root of *Panax notoginseng*, collected from Wenshan, Yunnan, China, and identified based on the DNA sequence (18S-ITSI-5.8S-ITS2-28S), which has been submitted to GenBank with accession number MH819653. BLAST search result revealed that the isolate belonged to the genus *Chaetomium* sp. with high identity (99%) to the species of *C. globosum*, and the fungus was deposited at the School of Life Science and Biopharmaceutics, Shenyang Pharmaceutical University.

Fermentation and extraction

Fermentation was carried out in Erlenmeyer flask (250 mL) each containing sterile water (53 mL) and rice (40 g) before sterilization at 121 °C for 30 min. The spore of *Chaetomium* sp. (2.0 mL) was inoculated in each Erlenmeyer flask (250 mL), then cultivated at 28 °C for 40 days. The fermented material was soaked with ethyl acetate (12 L) and the organic solvent was removed under reduced pressure to yield the crude extract (16.8 g), which was dissolved using 90% MeOH–H$_2$O (1 L) and extracted by cyclohexane (1 L) to obtain the residue (10.5 g).

Isolation and purification

The extract (10.5 g) was separated by silica gel for column chromatography (CC) eluted with petroleum ether–EtOAc (100 : 1 to 1 : 1) and CH$_2$Cl$_2$–MeOH (100 : 1 to 1 : 1), yielding eleven fractions (1–11). Fraction 5 (675.5 mg) was separated by C18-reversed phase silica gel CC using MeOH–H$_2$O gradient elution to afford three subfractions. Subfraction 5-2 (28.5 mg) was separated by preparative HPLC (CH$_3$CN–H$_2$O, 50%) to afford compound **7** (34.3 mg). Subfraction 5-3 (62.6 mg) was repeatedly crystalized with MeOH–H$_2$O at room temperature to yield compound **8** (2.0 mg). Fraction 6 (360.5 mg) was charged on Sephadex LH-20 column (200 mL) with MeOH as eluent to afford six subfractions. Subfraction 6-6 (150 mg) was separated by preparative HPLC with 60% CH$_3$CN–H$_2$O to yield compounds **9** (4.5 mg), **10** (7.2 mg) and **11** (5.1 mg). Compounds **6** (11.9 mg) and **12** (4.5 mg) were afforded from fraction 7 (430.2 mg) through C18-reversed phase silica gel CC with MeOH–H$_2$O gradient elution and preparative HPLC (CH$_3$CN–H$_2$O, 51%). Fraction 8 (477.8 mg) was crystalized with MeOH–H$_2$O at room temperature to afford compound **13** (36.5 mg). Fraction 9 (106.7 mg) was separated by Sephadex LH-20 gel filtration chromatography eluted with MeOH to five subfractions. Purification of subfraction 9-4 (70.0 mg) by preparative HPLC (CH$_3$CN–H$_2$O, 36%) led to the isolation of compound **3** (13.0 mg). Separation of fraction 10 (979.6 mg) by C18-reversed phase silica gel CC with MeOH–H$_2$O gradient elution afforded two subfractions. Finally, subfraction 10-1 (106.0 mg) was subject to preparative HPLC (CH$_3$CN–H$_2$O, 25%), which led to the isolation of compounds **1** (12 mg), **2** (7.9 mg), **4** (8.3 mg) and **5** (8.4 mg).

Chetoseminudin F (1). White powder; $[\alpha]_D^{20}$ −48.67 (*c* 0.5, MeOH); UV (MeOH) λ_{max} (log ε) 274, 281, and 290 nm; IR (KBr) ν_{max} 3380, 3225, 2923, 2851, 1677, 1641, 1448, 1434, 1386, 1287, 1265, 1242, 1207, 1155, 1099, 1025, 1011, 982, 923, 896, 877, 835, 772, 742, 725, 637, 626, 594, 566, 485, 429 cm^{-1}; ^{1}H (600 MHz, DMSO-d_6) and ^{13}C NMR (150 MHz, DMSO-d_6) data, see Table 1, Fig. S3 and S4;† HRESIMS *m/z* 386.1148 [M + Na]$^+$ (calcd for C$_{17}$H$_{21}$N$_3$NaO$_4$S, 471.1145).

Chetoseminudin G (2). White powder; $[\alpha]_D^{20}$ −2.8 (*c* 0.5, MeOH); UV (MeOH) λ_{max} (log ε) 274, 281, and 290 nm; IR (KBr) ν_{max} 3419, 2921, 2851, 1677, 1457, 1422, 1384, 1323, 1274, 1236, 1196, 1160, 1100, 1068, 1012, 955, 891, 745, 715, 647, 603, 557, 431 cm^{-1}; ^{1}H (600 MHz, DMSO-d_6) and ^{13}C NMR (150 MHz, DMSO-d_6) data, see Table 1, Fig. S15 and S16;† HRESIMS *m/z* 372.0982 [M + Na]$^+$ (calcd for C$_{16}$H$_{19}$N$_3$NaO$_4$S, 349.1096).

Chetoseminudin B (3). Amorphous light yellow powder; ^{1}H (600 MHz, DMSO-d_6) and ^{13}C NMR (150 MHz, DMSO-d_6) data, see Table S1 and Fig. S25–S27;† ESI-MS *m/z* 402.2 [M + Na]$^+$.

Chetoseminudin C (4). Amorphous light white powder; ^{1}H (600 MHz, DMSO-d_6) and ^{13}C NMR (150 MHz, DMSO-d_6) data, see Table S5 and Fig. S28–S30;† ESI-MS *m/z* 388.1 [M + Na]$^+$ and 364.4 [M − H]$^-$.

Chetoseminudin E (5). White powder; ^{1}H (600 MHz, DMSO-d_6) and ^{13}C NMR (150 MHz, DMSO-d_6) data, see Table S1 and Fig. S31–S33;† ESI-MS *m/z* 350.4 [M + H]$^+$.

Chaetocochin C (6). Amorphous light white powder; ^{1}H (600 MHz, CDCl$_3$) and ^{13}C NMR (150 MHz, CDCl$_3$) data, see Table S2 and Fig. S34–S36;† ESI-MS *m/z* 739.4 [M − H]$^-$.

3-*epi*-Aureonitol (7). Amorphous light white powder; ^{1}H (600 MHz, CDCl$_3$) and ^{13}C NMR (150 MHz, CDCl$_3$) data, see Table S3 and Fig. S37–S39;† ESI-MS *m/z* 268.5 [M + Na + K]$^+$.

Ergosterol (8). Amorphous light yellow powder; ^{1}H (600 MHz, CDCl$_3$) and ^{13}C NMR (150 MHz, CDCl$_3$) data, see Table S4 and Fig. S40–S42;† ESI-MS m/z 419.4 [M + Na]$^+$.

Chetomin A (9). Amorphous light yellow powder; ^{1}H (600 MHz, CDCl$_3$) and ^{13}C NMR (150 MHz, CDCl$_3$) data, see Table S6 and Fig. S43–S45;† ESI-MS m/z 797.4 [M + Na]$^+$.

Chetomin B (10). White powder; ^{1}H (600 MHz, CDCl$_3$) and ^{13}C NMR (150 MHz, CDCl$_3$) data, see Table S6 and Fig. S46–S48;† ESI-MS m/z 868.9 [M + Na + K]$^+$.

Chetomin C (11). Amorphous light yellow powder; ^{1}H (600 MHz, CDCl$_3$) and ^{13}C NMR (150 MHz, CDCl$_3$) data, see Table S6 and Fig. S49–S51;† ESI-MS m/z 861.9 [M + Na]$^+$.

Chetomin (12). Amorphous light white powder; ^{1}H (600 MHz, CDCl$_3$) and ^{13}C NMR (150 MHz, CDCl$_3$) data, see Table S6 and Fig. S52–S54;† ESI-MS m/z 711.6 [M + H]$^+$.

Dethiotetra-(methylthio)-chetomin (13). Amorphous light yellow powder; ^{1}H (600 MHz, CDCl$_3$) and ^{13}C NMR (150 MHz, CDCl$_3$) data, see Table S6 and Fig. S55–S57;† ESI-MS m/z 794.2 [M + Na]$^+$.

Antimicrobial assays

Compounds 1–13 were assayed for their antibacterial activities against *Staphylococcus aureus*, *Bacillus subtilis*, *Escherichia coli*, *Enterococcus faecium*, *Proteus mirabilis*, *Acinetobacter baumannii*, *Achromobacter marplatensis* and antifungal activity against *Candida albicans* according to our previous method.[19] Compounds 1–13 were dissolved in DMSO at an initial concentration at 10 mg mL^{-1}. Ampicillin, was used as a positive control. The *S. aureus*, *B. subtilis*, *E. coli*, *E. faecium*, *P. mirabilis*, *A. baumannii*, and *A. marplatensis* were preincubated at 37 °C for 24 h in Luria–Bertani (LB) media, respectively. *Candida albicans* was incubated at 28 °C for 48 h in PDA media. The bacterial suspension was diluted to the predetermined starting concentration OD$_{600}$ = 0.2. Then 1.0 mL bacterial solution was added into 24.0 mL LB media. The bacterial solution was transferred into a 96-well plate (198 μL per well) and the 2 μL of compounds 1–13. After 24 h cultivated, absorbance was determined at 600 nm by a microplate reader. Every experiment was performed in three biological replicates in triplicate to validate the screening method.

Antitumor assays

Human lung carcinoma cell A549 and human breast cancer cell MDA-MB-231, purchased from American Type Culture Collection (ATCC, Rockville, MD, USA), were cultured in DMEM medium, supplemented with 10% fetal bovine serum (Yuanheng Shengma Biology Technology Research Institute, Beijing, People's Republic of China), 100 U mL^{-1} penicillin, and 100 mg mL^{-1} streptomycin. Cultures were maintained in an incubator (NuAir, USA) with 5% CO$_2$ at 37 °C.

The viability of cells was performed using an MTT [3-(4,5-dimethylthiazol-2-yl)-2,5-diphenyltetrazolium bromide] (Sigma, USA) method in 96-well microplates, as reported previously,[37] with slight modification. Cells were plated in 96-well culture plates (93 103 per well) and allowed to adhere for 24 h before treated with fungal metabolites at a series of concentration (0,

0.5, 1, 5, 10, and 20 mg mL^{-1}) for 48 hours. Add 20 mL MTT (5 mg mL^{-1}) per well was added prior to 4 h incubation at 37 °C. Upon medium removal, formazans depositing on the plate were dissolved in 150 mL DMSO, then, the cell viability was detected by a Tecan microplate reader (Austria) at λ = 492 nm, and the IC$_{50}$ values were obtained from the MTT viability curves using GraphPad Prism 4.0.

Morphological observation of *B. subtilis* in the absence or presence of active compounds

To further study the possible antibacterial mechanism of the active compounds in more detail, the cells of *B. subtilis* were treated with the purified compounds, and observed using transmission electron microscopy (TEM, HT7700, Japan). *B. subtilis* cells were grown separately at 37 °C on agar plates and diluted with LB broth to an OD$_{600}$ value of 0.2. Compounds 6, 9 and 12 at the working concentrations of 0.5, 0.4 and 4.8 μg mL^{-1} (twice the MIC), respectively, were used to treat the *B. subtilis* cells. Samples of the treated cells and controls were cultivated at 37 °C for an additional 3 h. The bacterial suspensions were dyed with 2% phosphotungstic acid (1 : 1, v/v, pH 6.5) for 3–5 min, and a transmission scan was performed as previously described.[38]

Molecular docking

FtsZ is a prokaryotic homologue to the eukaryotic tubulin. Thus, molecular docking was used to investigate the interaction of FtsZ and the active compounds. The crystal structure of FtsZ from *B. subtilis* was obtained from the RCSB Protein Data Bank using the PDB Code 2VXY.[19] The protein structure was prepared using Discovery Studio 4.3 (Accelrys Inc., San Diego, USA). Water molecules were removed, and hydrogen atoms were added. The prepared structure was saved in the PDB format for docking studies. The 3D structures of the compounds were prepared and Gasteiger–Hückel charges were added using Sybyl software (Tripos, America). The ligand was subjected to energy minimization with Tripos force filed parameters.[39] Blind docking was conducted using the Molegro Virtual Docker 4.0 (Molegro ApS, Aarhus, Denmark) programme. The 3D docking grid was sufficiently large to cover the protein.

Conflicts of interest

The authors have no conflicts of interest with any parties or individuals.

Acknowledgements

References

1 L. Keyang, Z. Yisheng, L. Li, W. Xuewei and D. Gang, *Molecules*, 2013, **18**, 10944–10952.

2 W. B. Geiger, J. E. Conn and S. A. Waksman, *J. Bacteriol.*, 1944, **48**, 531–536.

3 C. Chen, J. Wang, J. Liu, H. Zhu, B. Sun, J. Wang, J. Zhang, Z. Luo, G. Yao and Y. Xue, *J. Nat. Prod.*, 2015, **78**, 1193–1201.

4 A. Pontius, A. Krick, S. Kehraus, R. Brun and G. M. König, *J. Nat. Prod.*, 2008, **71**, 1579–1584.

5 M. G. Hui, Y. Z. Wei, D. Gang, P. Saparpakorn, C. S. Yong, S. Hannongbua and X. T. Ren, *Chem. Commun.*, 2008, **40**, 5978–5980.

6 Q. L. Xu, Y. S. Xiao, Y. Shen, H. M. Wu, X. Zhang, X. Z. Deng, T. T. Wang, W. Li, R. X. Tan and R. H. Jiao, *J. Asian Nat. Prod. Res.*, 2017, **20**, 1–8.

7 J. Zhang, H. M. Ge, R. H. Jiao, J. Li, H. Peng, Y. R. Wang, J. H. Wu, Y. C. Song and R. X. Tan, *Planta Med.*, 2010, **76**, 1910–1914.

8 L. Xiang, T. Ye, Y. Sheng-Xiang, Z. Ya-Mei and Q. Jian-Chun, *Bioorg. Med. Chem. Lett.*, 2013, **23**, 2945–2947.

9 W. Li, X. Yang, Y. Yang, R. Duang, G. Chen, X. Li, Q. Li, S. Qin, S. Li and L. Zhao, *Nat. Prod. Res.*, 2016, **30**, 2616–2619.

10 T. X. D. Tina, X. M. Cui, Z. H. Song, J. Z. Kui, Z. N. Ji, C. K. Lo and W. K. T. Karl, *J. Agric. Food Chem.*, 2003, **51**, 4617–4623.

11 H. B. Guo, X. M. Cui, N. An and G. P. Cai, *Genet. Resour. Crop Evol.*, 2010, **57**, 453–460.

12 L. Ma, Y. H. Cao, M. H. Cheng, Y. Huang, M. H. Mo, Y. Wang, J. Z. Yang and F. X. Yang, *Antonie van Leeuwenhoek*, 2013, **103**, 299–312.

13 J. H. Lee, Y. H. Yu, Y. H. Kim, S. H. Ohh and W. M. Park, *Plant Pathol. J.*, 1990, **6**, 13–20.

14 Z. Y. Fan, C. P. Miao, X. G. Qiao, Y. K. Zheng, H. H. Chen, Y. W. Chen, L. H. Xu, L. X. Zhao and H. L. Guan, *J. Ginseng Res.*, 2016, **40**, 97–104.

15 A. A. Gunatilaka, *J. Nat. Prod.*, 2006, **69**, 509–526.

16 P. Chomcheon, S. Wiyakrutta, T. Aree, N. Sriubolmas, N. Ngamrojanavanich, C. Mahidol, S. Ruchirawat and P. Kittakoop, *Chem. Eur J.*, 2010, **16**, 11178–11185.

17 Y. N. An, X. Zhang, T. Y. Zhang, M. Y. Zhang, Q. Zhang, X. Y. Deng, F. Zhao, L. J. Zhu, G. Wang and J. Zhang, *Sci. Rep.*, 2016, **6**, 27396.

18 F. Wang, W. Zhao, C. Zhang, S. Chang, R. Shao, J. Xing, M. Chen, Y. Zhang and S. Si, *RSC Adv.*, 2019, **9**, 16035–16039.

19 J. Xie, Y. Y. Wu, T. Y. Zhang, M. Y. Zhang, F. Peng, B. Lin and Y. X. Zhang, *Fitoterapia*, 2018, **131**, 35–43.

20 D. W. Adams and E. Jeff, *Nat. Rev. Microbiol.*, 2009, **7**, 642–653.

21 J. Errington, R. A. Daniel and D. J. Scheffers, *Microbiol. Mol. Biol. Rev.*, 2003, **67**, 52–65.

22 M. G. Pinho and J. Errington, *Mol. Microbiol.*, 2010, **50**, 871–881.

23 N. R. Stokes, N. Baker, J. M. Bennett, J. Berry, I. Collins, L. G. Czaplewski, A. Logan, R. Macdonald, L. Macleod and H. Peasley, *Antimicrob. Agents Chemother.*, 2013, **57**, 317–325.

24 F. Q. Wang, Q. Y. Tong, H. R. Ma, H. F. Xu, S. Hu, W. Ma, Y. B. Xue, J. J. Liu, J. P. Wang and H. P. Song, *Sci. Rep.*, 2015, **5**, 9294.

25 H. Fujimoto, M. Sumino, E. Okuyama and M. Ishibashi, *J. Nat. Prod.*, 2004, **67**, 98–102.

26 I. Marmouzi, M. E. A. Faouzi, N. Saidi, Y. Cherrah, N. Rehberg, S. S. Ebada, W. Ebrahim, R. Kalscheuer and P. Proksch, *Chem. Nat. Compd.*, 2017, **6**, 1208–1211.

27 G. Y. Li, B. G. Li, T. Yang, J. F. Yan, A. G. Y. Liu and G. L. Zhang, *J. Nat. Prod.*, 2006, **69**, 1374–1376.

28 R. G. Marwah, M. O. Fatope, M. L. Deadman, Y. M. Al-Maqbali and J. Husband, *ChemInform*, 2007, **63**, 8174–8180.

29 H. C. Kwon, S. D. Zee, S. Y. Cho, S. U. Choi and K. R. Lee, *Arch. Pharmacal Res.*, 2002, **25**, 851–855.

30 M. H. Wang, Y. C. Hu, B. D. Sun, M. Yu, S. B. Niu, Z. Guo, X. Y. Zhang, T. Zhang, G. Ding and Z. M. Zou, *Org. Lett.*, 2018, **20**, 1806–1809.

31 T. R. Welch and R. M. Williams, *Tetrahedron*, 2013, **69**, 770–773.

32 D. H. Scharf, T. Heinekamp, N. Remme, P. Hortschansky, A. A. Brakhage and C. Hertweck, *Appl. Microbiol. Biotechnol.*, 2012, **93**, 467–472.

33 C. Davis, S. Carberry, M. Schrettl, I. Singh, J. Stephens, S. Barry, K. Kavanagh, G. Challis, D. Brougham and S. Doyle, *Chem. Biol.*, 2011, **18**, 542–552.

34 B. Li, R. R. Forseth, A. A. Bowers, F. C. Schroeder and C. T. Walsh, *ChemBioChem*, 2012, **13**, 2521–2526.

35 N. Timothy, C. A. Lewis, K. J. Eastman and P. S. Baran, *J. Am. Chem. Soc.*, 2010, **132**, 7119–7137.

36 R. L. Lock and E. J. Harry, *Nat. Rev. Drug Discovery*, 2008, **7**, 324–338.

37 Z. Luo, F. Wang, J. Zhang, X. Li, M. Zhang, X. Hao, Y. Xue, Y. Li, F. D. Horgen and G. Yao, *J. Nat. Prod.*, 2012, **75**, 2113–2120.

38 P. Sass, M. Josten, K. Famulla, G. Schiffer, H. G. Sahl, L. Hamoen and H. Brötzoesterhelt, *Proc. Natl. Acad. Sci. U. S. A.*, 2011, **108**, 17474–17479.

39 S. Ballu, R. Itteboina, S. K. Sivan and V. Manga, *J. Recept. Signal Transduction Res.*, 2018, **38**, 61–70.